Scaling of diffusion constants in the spin-$\frac{1}{2}$ XX ladder

R. Steinigeweg,[1,*] F. Heidrich-Meisner,[2] J. Gemmer,[3] K. Michielsen,[4,5] and H. De Raedt[6]

[1]*Institute for Theoretical Physics, Technical University Braunschweig, D-38106 Braunschweig, Germany*

[2]*Department of Physics and Arnold Sommerfeld Center for Theoretical Physics, Ludwig-Maximilians-Universität München, D-80333 Munich, Germany*

[3]*Department of Physics, University of Osnabrück, D-49069 Osnabrück, Germany*

[4]*Institute for Advanced Simulation, Jülich Supercomputing Centre, Forschungszentrum Jülich, D-52425 Jülich, Germany*

[5]*RWTH Aachen University, D-52056 Aachen, Germany*

[6]*Department of Applied Physics, Zernike Institute for Advanced Materials, University of Groningen, NL-9747AG Groningen, Netherlands*

(Received 13 June 2014; revised manuscript received 11 September 2014; published 25 September 2014)

We study the dynamics of spin currents in the spin-$\frac{1}{2}$ XX ladder at finite temperature. Within linear response theory, we numerically calculate autocorrelation functions for quantum systems larger than what is accessible with exact diagonalization using the concept of dynamical quantum typicality. While the spin Drude weight vanishes exponentially quickly with increasing system size, we show that this model realizes standard diffusive dynamics. Moreover, we unveil the existence of three qualitatively different dependencies of the spin-diffusion coefficient on the rung-coupling strength, resulting from a crossover from exponential to Gaussian dissipation as the rung coupling increases, in agreement with analytical predictions. We further discuss the implications of our results for experiments with cold atomic gases.

DOI: 10.1103/PhysRevB.90.094417 PACS number(s): 75.10.Jm, 05.60.Gg, 71.27.+a

I. INTRODUCTION

The theoretical understanding of transport properties of interacting quantum many-body systems is paramount in characterizing states of matter. Strongly interacting one-dimensional (1D) systems may exhibit either diffusive or ballistic transport properties at finite temperatures [1–4], the latter being due to local conservation laws in integrable models [1,5–8]. These unusual properties have been speculated to be related to the huge magnetic thermal conductivities observed in 1D quantum magnets [9–11] and may have potential applications in signal propagation in artificial 1D systems on surfaces [12] or for spintronics applications [13,14]. Generic nonintegrable 1D systems are believed to exhibit no ballistic dynamics [15–18] and presumably diffusive transport (see Refs. [19–22] for possible exceptions or corrections beyond diffusion). Recent experimental studies on 1D quantum magnets have set out to elucidate spin diffusion using muon spin relaxation and NMR [23,24].

More recently, it has become possible to address qualitative aspects of mass transport in experiments with ultracold quantum gases in optical lattices [25–27] based on the realization of Bose- and Fermi-Hubbard models in these systems [28]. Sudden-expansion experiments, using the release of a trapped gas of atoms into an empty and homogeneous optical lattice, suggest that mass transport in two-dimensional (2D) Hubbard models is diffusive for both bosons and fermions [25,26]. Bosons in 1D subject to infinitely strong interactions, called hard-core bosons, however, are integrable via the exact mapping to noninteracting fermions [29], and the results of [26] establish an unambiguous experimental realization of ballistic dynamics in an integrable 1D system, rendering this a suitable starting point for future studies. Moreover, hard-core bosons are equivalent to spin-$\frac{1}{2}$ XX models [29], thus providing a connection to research on the transport properties of quantum magnets.

An important question concerns the effect of integrability breaking on transport properties. In quantum gas experiments, a straightforward way to break integrability is to induce an interchain coupling, and indeed, experimental results for sudden expansions in the 1D-2D crossover of interacting bosons indicate a rapid emergence of diffusive-like behavior upon increasing the interchain coupling [26].

As an alternative to the dimensional crossover, one can consider two coupled chains, i.e., a ladder, which can easily be realized in optical lattices using superlattices [30]. The ladder is accessible to state-of-the-art numerical methods, while for two-dimensional systems, there are no reliable approaches. The first studies of the dynamics of hard-core bosons on a ladder geometry in the sudden expansion [31] or for wave-packet dynamics [32] indicate diffusive dynamics for sufficiently large interchain coupling, yet a rigorous analysis of ballistic and diffusive contributions based on linear response theory is lacking.

In this work, we address precisely this question using the spin-$\frac{1}{2}$ XX ladder. By exploiting the concept of dynamical quantum typicality [33–37], we are able to study ladders with up to $N \leqslant 36$ spins, going beyond the range of exact diagonalization. In addition, we can reach the long time scales required to analyze ballistic contributions [36]. In the high-temperature limit, we first demonstrate the absence of ballistic contributions, and we show that the model realizes standard diffusive dynamics; that is, there is a single relaxation time. We further compute the diffusion constant as a function of the interchain coupling, and as another main result, we identify three regimes characterized by qualitatively different time dependencies of current autocorrelation functions. Finally, we discuss a possible experiment with quantum gases that could put our theoretical predictions to the test.

*r.steinigeweg@tu-bs.de

The plan of this paper is the following: In Sec. II, we introduce the Hamiltonian and define the quantities of interest, namely, the spin-current autocorrelation function, the Drude weight, and the diffusion constant. In Sec. III, we briefly discuss the numerical method, which is based on the concept of dynamical typicality. Section IV contains our main results for the time dependence of the spin-current autocorrelation, the finite-size scaling of the ballistic contribution, and the diffusion constant. We also discuss our results in the context of recent quantum gas experiments with interacting bosons in optical lattices and make a proposal for a future experiment designed to observe our predictions. Our conclusions are presented in Sec. V.

II. MODEL AND DEFINITIONS

We study spin-current dynamics in an XX ladder of length $N/2$ with periodic boundary conditions, where N is the number of sites. The Hamiltonian $H = J_{\parallel} H_{\parallel} + J_{\perp} H_{\perp}$ consists of a leg part $H_{\parallel}$ and rung part $H_{\perp}$, given by ($\hbar = 1$)

$$H_{\parallel} = \sum_{i=1}^{N/2} \sum_{k=1}^{2} \left(S^x_{i,k} S^x_{i+1,k} + S^y_{i,k} S^y_{i+1,k} \right),$$
$$H_{\perp} = \sum_{i=1}^{N/2} \left(S^x_{i,1} S^x_{i,2} + S^y_{i,1} S^y_{i,2} \right), \tag{1}$$

where $S^{x,y}_{i,k}$ are spin-$\frac{1}{2}$ operators at site (i,k), $J_{\parallel} > 0$ is the antiferromagnetic exchange coupling constant along the legs, and $J_{\perp} = r\, J_{\parallel} > 0$ is the strength of the rung coupling. While the XX ladder splits into two integrable XX chains of free Jordan-Wigner fermions for $r = 0$, it simplifies to a set of uncoupled dimers for $r \to \infty$. In the case of $r \neq 0$, the XX ladder is nonintegrable, and the Jordan-Wigner transformation maps hard-core bosons to interacting fermions [31]. In general, the model in Eq. (1) preserves the total magnetization S^z and is invariant under translations with periodic boundary conditions. We take into account the full Hilbert space with $d = 2^N$ states and focus on the case for which $\langle S^z \rangle = 0$ (see Sec. IV D).

The longitudinal spin current is defined via the continuity equation and has the form

$$j = J_{\parallel} \sum_{i=1}^{N/2} \sum_{k=1}^{2} \left(S^x_{i,k} S^y_{i+1,k} - S^y_{i,k} S^x_{i+1,k} \right). \tag{2}$$

$[H, j] = 0$ holds only at $r = 0$. Within linear response theory, we are interested in the current autocorrelation function at inverse temperatures $\beta = 1/T$ ($k_B = 1$),

$$C(t) = \mathrm{Re} \frac{\langle j(t)\, j \rangle}{N} = \mathrm{Re} \frac{\mathrm{Tr}\{e^{-\beta H} j(t)\, j\}}{N\, \mathrm{Tr}\{e^{-\beta H}\}}, \tag{3}$$

where the time argument of j has to be understood with respect to the Heisenberg picture, $j = j(0)$, and $C(0) = J_{\parallel}^2/8$ in the limit $\beta \to 0$. From this autocorrelation we obtain the two central quantities

$$\overline{C} = \frac{1}{t_2 - t_1} \int_{t_1}^{t_2} dt\, C(t), \quad D = \frac{1}{\chi} \int_0^{t_2} dt\, C(t), \tag{4}$$

with $t_2 > t_1$ and $t_2 \to \infty$. The first quantity, $\overline{C}$, is the spin Drude weight, which, being the nondecaying part of $C(t)$, signals ballistic transport [1]. The second quantity, D, is the spin-diffusion constant, well defined for a vanishing $\overline{C}$ [and a sufficiently fast decay of $C(t)$]. The prefactor χ is the static susceptibility (per spin), and $\chi = 1/4$ as $\beta \to 0$. The numerical calculation of the two quantities in Eq. (4) is feasible by choosing finite but sufficiently long times t_1 and t_2, where $C(t)$ has already decayed to its final value, and $t_2 \gg t_1$.

III. NUMERICAL METHOD: DYNAMICAL TYPICALITY

Our numerical method relies on replacing the trace $\mathrm{Tr}\{\bullet\} = \sum_n \langle n| \bullet |n\rangle$ in Eq. (3) by a scalar product involving a single pure state $|\psi\rangle$. More precisely, following the concept of quantum typicality, we draw $|\psi\rangle$ at random according to a probability distribution that is invariant under all possible unitary transformations in Hilbert space (Haar measure). Using a so-constructed $|\psi\rangle$ and abbreviating $|\psi_\beta\rangle = e^{-\beta H/2}|\psi\rangle$, the autocorrelation function in Eq. (3) is approximated by [33–37]

$$C(t) \approx \mathrm{Re} \frac{\langle \psi_\beta | j(t)\, j | \psi_\beta \rangle}{N\, \langle \psi_\beta | \psi_\beta \rangle}, \tag{5}$$

with the approximation becoming more accurate as the dimension of the Hilbert space increases [36,38].

The salient feature of Eq. (5) is that it can be calculated numerically without diagonalization of the Hamiltonian. To this end one has to introduce two pure states: The first reads $|\Phi_\beta(t)\rangle = e^{-\imath Ht - \beta H/2}\, |\psi\rangle$, and the second is $|\varphi_\beta(t)\rangle = e^{-\imath Ht}\, j\, e^{-\beta H/2}\, |\psi\rangle$. Then,

$$\langle \psi_\beta | j(t)\, j | \psi_\beta \rangle = \langle \Phi_\beta(t) | j | \varphi_\beta(t) \rangle. \tag{6}$$

The dependence of the two states on t and β is calculated numerically by a massively parallel implementation of a Suzuki-Trotter product formula or Chebyshev polynomial algorithm. This allows us to study quantum systems with as many as $N = 36$ spins [Hilbert-space dimension $d = O(10^{11})$], although we do not exploit symmetries of Eqs. (1) and (2) at present [36].

IV. RESULTS

A. Time dependence of current autocorrelations

We begin with high temperatures $\beta \to 0$ and an intermediate rung interaction strength $r = 1$. Figure 1(a) summarizes our numerical results for $C(t)$ for different system sizes $N = 20$, 24, 28, and 36. Clearly, $C(t)$ rapidly decays towards zero for all N, with almost no finite-size effects visible in the lin-lin plot. Particularly, for all N depicted, there is no signature of a dissipationless contribution of $C(t)$ for times $t\, J_{\parallel} \leqslant 50$. To illustrate the existence of such a contribution, Fig. 1(b) shows a semilog plot of $C(t)$ up to times $t\, J_{\parallel} \leqslant 400$. Although a dissipationless contribution becomes visible, it amounts to only 1% of the initial value $C(0)$ for $N = 20$ and systematically decreases further when N is increased, taking a tiny value $\ll 1\%$ for $N = 28$. Note that we do not determine $\bar{C}$ for larger N since, for such N, the computational effort is unreasonably high for the long times $t\, J_{\parallel} > 400$ required.

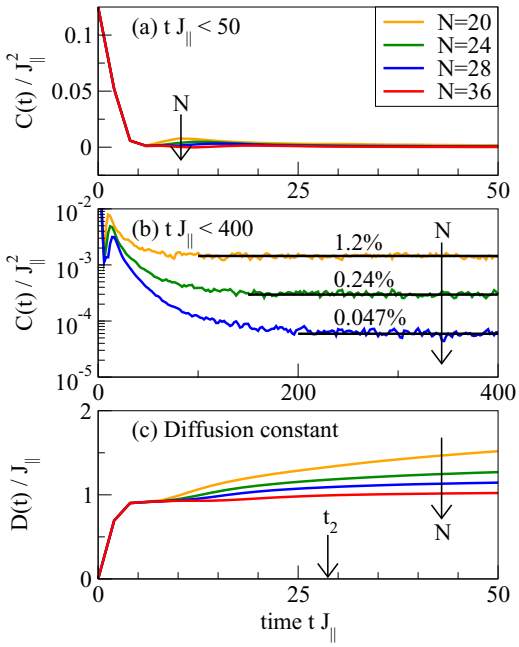

FIG. 1. (Color online) Spin-current autocorrelation function $C(t)$ for $r = J_\perp/J_\parallel = 1$ and $\beta = 0$: (a) Relaxation curve for large systems $N \leqslant 36$ and times $t\,J_\parallel \leqslant 50$. (b) Saturation at a very small Drude weight is only visible in a semilog plot of (a) for very long times $t\,J_\parallel \gg 50$. (c) Since the Drude weight $\overline{C} \lesssim O(1\%)$, $D(t) \to$ const for large times.

B. Absence of ballistic contributions for large N

In Fig. 2 we provide a detailed finite-size analysis of the nondecaying contribution based on system sizes where this contribution can be extracted from the long-time window $[t_1 J_\parallel, t_2 J_\parallel] = [300,400]$; see Fig. 1(b) as well as the definition of $\overline{C}$ in Eq. (4). Using a log-lin plot unveils an exponential decrease with system size, over more than two orders of magnitude. Certainly, this kind of decrease may be expected for a highly nonintegrable model [37], but we observe this scaling for various rung couplings $r = 0.25$, 0.5, 0.75, and 1. What is more, the exponent turns out to be practically independent of r, while the amplitude scales roughly as $\propto 1/r$. Based on these results, we conclude that, for $r > 0$, the Drude weight vanishes in the thermodynamic limit. Compared to earlier studies of transport in gapped 1D spin systems [15–18], we resolve a

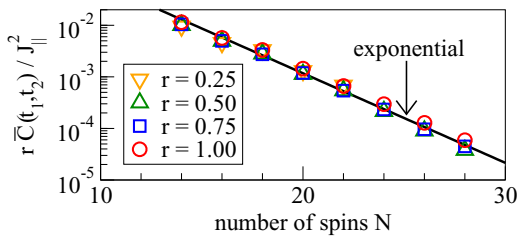

FIG. 2. (Color online) High-temperature spin Drude weight $\overline{C}(t_1,t_2)$, extracted at very long times $[t_1 J_\parallel, t_2 J_\parallel] = [300,400]$, for different coupling ratios $r = J_\perp/J_\parallel = 0.25$, 0.5, 0.75, and 1 (symbols). The finite-size scaling follows an exponential $A(r)\,e^{-\gamma N}$ [solid line, $\gamma \neq \gamma(r)$ and $A(r) = 1/r$], suggesting $\overline{C} \to 0$ for $N \to \infty$.

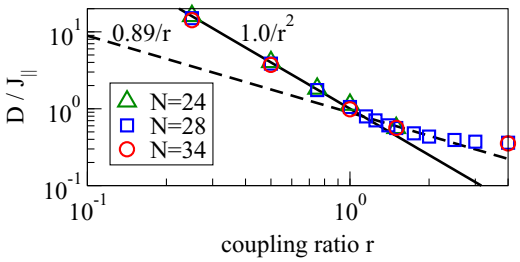

FIG. 3. (Color online) Spin-diffusion constant D vs $r = J_\perp/J_\parallel$ for $\beta \to 0$. There are apparently three scaling regimes: (i) $r \ll 1$: $D \propto 1/r^2$, (ii) $1 \lesssim r \lesssim 2$: $D \propto 1/r$, and (iii) $r \gg 1$: $D =$ const. The $1/r$ curve results from Eq. (7); see text.

particularly clean exponential and fast decay of the Drude weight.

C. Diffusion constant

Since the Drude weight vanishes, the central quantity of interest is the diffusion constant. In fact, we are able to calculate the diffusion constant even quantitatively using large systems due to the tiny nondecaying contribution for such systems. Still, we have to choose a finite time t_2 for the evaluation of D in Eq. (4). In praxis, we determine the decay time τ, where $C(\tau)/C(0) = 1/e$, and calculate D for $t_2 = 5.5\tau \gg \tau$. For instance, from the data shown for $r = 1$ in Fig. 1(c), we get $t_2\,J_\parallel \approx 28$ and therefore a reasonable choice of t_2 with little finite-size effects for large N. Note that we cannot choose extremely long t_2, which would artificially blow up tiny nondecaying contributions or include other finite-size effects. In Fig. 3 we depict the resulting quantitative values of the diffusion constant as a function of the rung coupling r. Values for different N exhibit little finite-size effects for all r. The log-log plot clearly unveils several regimes with a power-law dependence of D on r. More precisely, we observe three qualitatively different regimes: (i) $r \ll 1$, where $D \propto 1/r^2$, (ii) $1 \lesssim r \lesssim 2$, where $D \propto 1/r$, and (iii) $r \gg 1$, where $D =$ const. The intermediate regime (ii) is notably much narrower than regimes (i) and (iii) yet distinct by the $D \propto 1/r$ scaling. Note that in the XXZ chain similar regimes appear as a function of the exchange anisotropy [32,39,40].

To gain insight into the origin of the scaling of D with r, we consider the time dependence of the spin-current autocorrelation function $C(t)$ in more detail. In Fig. 4(a) we show $C(t)$ for a weak rung coupling $r = 0.25$. Evidently, the time dependence of $C(t)$ is well described by a simple exponential relaxation, implying standard diffusion. Due to this exponential relaxation and the scaling $D \propto 1/r^2$ in Fig. 3, the weak $r \ll 1$ regime turns out to be a conventional perturbative regime [39,40]. For $r > 1$ the behavior changes qualitatively. In Fig. 4(b) we depict $C(t)$ for $r = 1.5$. Here the exponential relaxation turns into a Gaussian decay. This kind of decay, and particularly the scaling $D \propto 1/r$ evident from Fig. 3, is in line with the generic behavior suggested in [39,40] for the case of strong perturbations. In fact, according to Ref. [40], one expects at high temperatures $\beta \to 0$

$$C(t) = C(0)\,e^{-r^2\gamma t^2}, \quad \gamma = \frac{\mathrm{Tr}\{\imath[j,H_\perp]^2\}}{\mathrm{Tr}\{j^2\}} = \frac{1}{4}, \qquad (7)$$

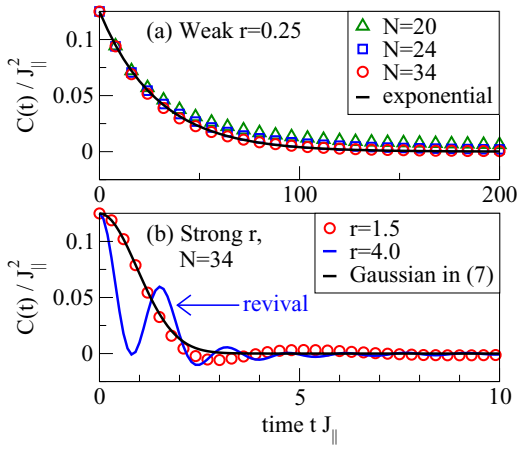

FIG. 4. (Color online) Spin-current autocorrelation function $C(t)$ for $\beta \to 0$: qualitatively different regimes, depending on $r = J_\perp/J_\parallel$. (a) Weak-r regime: $C(t)$ decays exponentially, resulting in $D \propto 1/r^2$, as expected from perturbation theory. (b) Strong-r regime: The decay curve agrees with the Gaussian prediction of Eq. (7), in line with the generic behavior $D \propto 1/r$ suggested in Refs. [39,40]. For large r, revivals occur, resulting in $D = \text{const}$.

and therefore, $D = C(0)\sqrt{\pi}/(2r\chi\sqrt{\gamma}) \approx 0.89/r$. The prediction of Eq. (7) is in good agreement with the numerical data for $C(t)$ at $r = 1.5$ shown in Fig. 4(b). However, it does not account for possible revivals of $C(t)$ that occur in our case because of the bandlike spectrum that emerges in the limit of strong rung dimers for $r \to \infty$. In this limit (r large but finite), transport is mediated by the triplet excitations above the dimer ground state [10]. In Fig. 4(b) we illustrate the onset of such revivals for $r = 4$. These revivals define the third regime with $D = \text{const}$ shown in Fig. 3, in analogy to the spin-$\frac{1}{2}$ XXZ chain, where a similar behavior emerges in the vicinity of the Ising limit [32]. The observation of diffusive transport with a single relaxation time and the identification of the three scaling regimes characterized by qualitatively different decays of current autocorrelations constitute the main results of this work.

D. Finite temperatures and finite magnetization

The qualitative dependence of D on r depends on temperature (see, e.g., Ref. [41] for a theory of diffusion in 1D gapped quantum magnets at low T). In Fig. 5, we check for the three different r regimes that the qualitative decay of $C(t)$ does not change down to $T/J_\parallel \sim 2$, and hence, it is reasonable to expect no qualitative changes in the r dependence of D. In Fig. 6, we check that a finite magnetization $S^z \sim 0$ does not change the picture either. We note that the small differences between $\langle S^z\rangle = 0$, $S^z = 0$, and $S^z = 1$ visible in Fig. 6 are finite-size effects and vanish in the thermodynamic limit $N \to \infty$ (see Fig. 7). Remarkably, the convergence to that limit is the fastest for $\langle S^z\rangle = 0$, which is the reason for focusing on this ensemble in our paper.

E. Connection to quantum gas experiments

With respect to the recent sudden expansion experiment [26] of strongly interacting bosons on coupled chains,

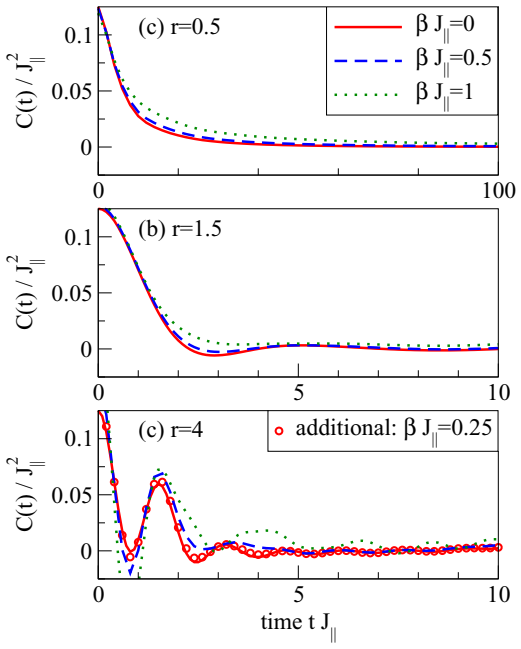

FIG. 5. (Color online) Spin-current autocorrelation function $C(t)$ in the XX ladder for rung couplings (a) $r = 0.5$, (b) $r = 1.5$, and (c) $r = 4$ and different temperatures $\beta J_\parallel \leqslant 1$. In all cases, $N = 28$. Apparently, $C(t)$ is qualitatively the same for temperatures down to $\beta J_\parallel \sim 0.5$.

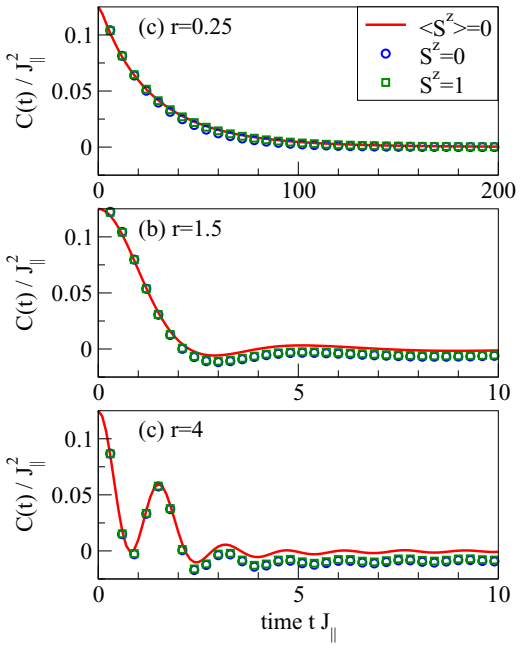

FIG. 6. (Color online) Spin-current autocorrelation function $C(t)$ in the XX ladder for rung couplings (a) $r = 0.25$, (b) $r = 1.5$, and (c) $r = 4$ in the high-temperature limit $\beta \to 0$ and $\langle S^z\rangle = 0$, $S^z = 0$, $S^z = 1$. In all cases, $N = 34$. Apparently, the cases of half filling $S^z = 0$ and almost half filling $S^z = 1$ are already practically identical for finite N. No significant difference from $\langle S^z\rangle = 0$ is visible for $r = 0.25$, while differences for larger r are finite-size effects, as illustrated in Fig. 7.

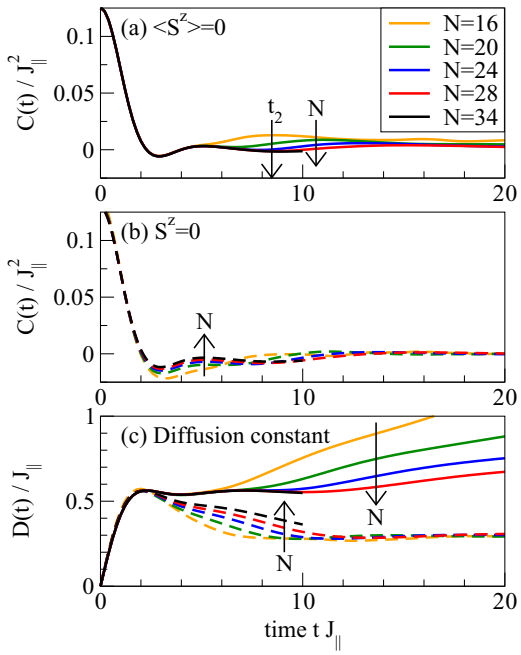

FIG. 7. (Color online) Spin-current autocorrelation function $C(t)$ in the XX ladder for (a) $\langle S^z\rangle = 0$ and (b) $S^z = 0$ for a strong rung coupling $r = J_\perp/J_\parallel = 1.5$ in the high-temperature limit $\beta \to 0$. (c) The resulting time-dependent diffusion coefficient, as extracted from $C(t)$ depicted in (a) and (b). Although finite-size results for $\langle S^z\rangle = 0$ and $S^z = 0$ differ from each other, they seem to converge to the same value in the thermodynamic limit. Apparently, the convergence of the $\langle S^z\rangle = 0$ data is much faster in time, and there are no finite-size effects up to times $t\ J_\parallel \sim 10$ when comparing $N = 28$ and $N = 34$. Hence, our choice of $t_2\ J_\parallel = 8.3$ for extracting D from $D(t)$ is reasonable.

we have here provided theoretical evidence that such systems indeed exhibit diffusive dynamics. Finally, we describe an experiment with cold quantum gases in which our quantitative results for the diffusion constant could be verified. Spin-$\frac{1}{2}$ XX models can be realized with a single-component Bose gas in an optical lattice in the limit of infinitely strong repulsive on-site interactions [26,42]. In order to probe diffusion, one would desire a homogeneous background density with half a particle per site, which could be accomplished by using a box trap [43] instead of harmonic trapping potentials. The basic idea to measure D is to induce a local perturbation in the density by, e.g., superimposing a dimple trap using methods along the lines of those in [44] and then to monitor the time evolution of the density profile as a function of position. From such information, one can extract the diffusion constant from the time dependence of the variance, as demonstrated for 1D spin systems [32,45]. In order to observe our predictions, it is necessary to put the gas at sufficiently high temperatures. This can be done by subjecting the gas to heating.

V. CONCLUSIONS

We studied spin transport in the spin-$\frac{1}{2}$ XX ladder at finite temperature. Within linear response theory and using the concept of dynamical typicality, this simple and experimentally realizable nonintegrable model exhibits standard diffusive dynamics. We found qualitatively different dependencies of the spin-diffusion constant on the rung-interaction strength, resulting from a crossover from exponential to Gaussian dissipation at intermediate coupling strengths. Our results suggest that strongly interacting bosons on coupled chains, studied experimentally in [26], exhibit diffusive dynamics.

ACKNOWLEDGMENTS

We thank U. Schneider for helpful discussions. F.H.-M. acknowledges support from the DFG through FOR 912 via Grant No. HE-5242/2-2. The authors gratefully acknowledge the computing time granted by the JARA-HPC Vergabegremium and provided on the JARA-HPC Partition part of the supercomputer JUQUEEN at Forschungszentrum Jülich.

[1] X. Zotos, F. Naef, and P. Prelovšek, Phys. Rev. B **55**, 11029 (1997).
[2] F. Heidrich-Meisner, A. Honecker, and W. Brenig, Eur. J. Phys. Spec. Top. **151**, 135 (2007).
[3] M. Žnidarič, Phys. Rev. Lett. **106**, 220601 (2011).
[4] R. Steinigeweg and W. Brenig, Phys. Rev. Lett. **107**, 250602 (2011).
[5] A. Rosch and N. Andrei, Phys. Rev. Lett. **85**, 1092 (2000).
[6] J. Sirker, R. G. Pereira, and I. Affleck, Phys. Rev. B **83**, 035115 (2011).
[7] T. Prosen, Phys. Rev. Lett. **106**, 217206 (2011).
[8] T. Prosen and E. Ilievski, Phys. Rev. Lett. **111**, 057203 (2013).
[9] A. V. Sologubenko, T. Lorenz, H. R. Ott, and A. Freimuth, J. Low Temp. Phys. **147**, 387 (2007).
[10] C. Hess, Eur. Phys. J. Spec. Top. **151**, 73 (2007).
[11] N. Hlubek, P. Ribeiro, R. Saint-Martin, A. Revcolevschi, G. Roth, G. Behr, B. Büchner, and C. Hess, Phys. Rev. B **81**, 020405 (2010).
[12] M. Menzel, Y. Mokrousov, R. Wieser, J. E. Bickel, E. Vedmedenko, S. Blügel, S. Heinze, K. von Bergmann, A. Kubetzka, and R. Wiesendanger, Phys. Rev. Lett. **108**, 197204 (2012).
[13] B. Trauzettel, P. Simon, and D. Loss, Phys. Rev. Lett. **101**, 017202 (2008).
[14] K. A. van Hoogdalem and D. Loss, Phys. Rev. B **84**, 024402 (2011).
[15] F. Heidrich-Meisner, A. Honecker, D. C. Cabra, and W. Brenig, Phys. Rev. B **68**, 134436 (2003).
[16] F. Heidrich-Meisner, A. Honecker, D. C. Cabra, and W. Brenig, Phys. Rev. Lett. **92**, 069703 (2004).
[17] P. Jung, R. W. Helmes, and A. Rosch, Phys. Rev. Lett. **96**, 067202 (2006).
[18] X. Zotos, Phys. Rev. Lett. **92**, 067202 (2004).
[19] C. Karrasch, R. Ilan, and J. E. Moore, Phys. Rev. B **88**, 195129 (2013).
[20] M. Žnidarič, Phys. Rev. Lett. **110**, 070602 (2013).

[21] R. Steinigeweg and T. Prosen, Phys. Rev. E **87**, 050103 (2013).
[22] R. Steinigeweg, H.-P. Breuer, and J. Gemmer, Phys. Rev. Lett. **99**, 150601 (2007).
[23] H. Maeter, A. A. Zvyagin, H. Luetkens, G. Pascua, Z. Shermadini, R. Saint-Martin, A. Revcolevschi, C. Hess, B. Büchner, and H.-H. Klauss, J. Phys.: Condens. Matter **25**, 365601 (2013).
[24] F. Xiao, J. S. Möller, T. Lancaster, R. C. Williams, F. L. Pratt, S. J. Blundell, D. Ceresoli, A. M. Barton, and J. L. Manson, arXiv:1406.3202.
[25] U. Schneider, L. Hackermüller, J. P. Ronzheimer, S. Will, S. Braun, T. Best, I. Bloch, E. Demler, S. Mandt, D. Rasch, and A. Rosch, Nat. Phys. **8**, 213 (2012).
[26] J. P. Ronzheimer, M. Schreiber, S. Braun, S. S. Hodgman, S. Langer, I. P. McCulloch, F. Heidrich-Meisner, I. Bloch, and U. Schneider, Phys. Rev. Lett. **110**, 205301 (2013).
[27] T. Fukuhara, A. Kantian, M. Endres, M. Cheneau, P. Schauß, S. Hild, C. Gross, U. Schollwöck, T. Giamarchi, I. Bloch, and S. Kuhr, Nat. Phys. **9**, 235 (2013).
[28] I. Bloch, J. Dalibard, and W. Zwerger, Rev. Mod. Phys. **80**, 885 (2008).
[29] M. A. Cazalilla, R. Citro, T. Giamarchi, E. Orignac, and M. Rigol, Rev. Mod. Phys. **83**, 1405 (2011).
[30] S. Fölling, S. Trotzky, P. Cheine, M. Feld, R. Saers, A. Widera, T. Mueller, and I. Bloch, Nature (London) **448**, 1029 (2007).
[31] L. Vidmar, S. Langer, I. P. McCulloch, U. Schneider, U. Schollwöck, and F. Heidrich-Meisner, Phys. Rev. B **88**, 235117 (2013).
[32] C. Karrasch, J. E. Moore, and F. Heidrich-Meisner, Phys. Rev. B **89**, 075139 (2014).
[33] A. Hams and H. De Raedt, Phys. Rev. E **62**, 4365 (2000).
[34] C. Bartsch and J. Gemmer, Phys. Rev. Lett. **102**, 110403 (2009).
[35] T. A. Elsayed and B. V. Fine, Phys. Rev. Lett. **110**, 070404 (2013).
[36] R. Steinigeweg, J. Gemmer, and W. Brenig, Phys. Rev. Lett. **112**, 120601 (2014).
[37] R. Steinigeweg, A. Khodja, H. Niemeyer, C. Gogolin, and J. Gemmer, Phys. Rev. Lett. **112**, 130403 (2014).
[38] F. Jin, H. De Raedt, S. Yuan, M. I. Katsnelson, S. Miyashita, and K. Michielsen, J. Phys. Soc. Jpn. **79**, 124005 (2010).
[39] R. Steinigeweg and R. Schnalle, Phys. Rev. E **82**, 040103 (2010).
[40] R. Steinigeweg, Phys. Rev. E **84**, 011136 (2011).
[41] K. Damle and S. Sachdev, Phys. Rev. Lett. **95**, 187201 (2005).
[42] B. Paredes, A. Widera, V. Murg, O. Mandel, S. Fölling, I. Cirac, G. V. Shlyapnikov, T. W. Hänsch, and I. Bloch, Nature **429**, 277 (2004).
[43] A. L. Gaunt, T. F. Schmidutz, I. Gotlibovych, R. P. Smith, and Z. Hadzibabic, Phys. Rev. Lett. **110**, 200406 (2013).
[44] N. Friedman, A. Kaplan, and N. Davidson, Adv. At. Mol. Opt. Phys. **48**, 99 (2002).
[45] S. Langer, F. Heidrich-Meisner, J. Gemmer, I. P. McCulloch, and U. Schollwöck, Phys. Rev. B **79**, 214409 (2009).